Medicinal Plants
Vol. 15 (4), December 2023, 677-690

doi : 10.5958/0975-6892.2023.00068.0

Research Article

Efficacy of methanolic extract of *Zingiber officinale* against seed-born fungi

Navoda Hansini[1], A.M.S.C. Sooriyawansha[2], P.A.S.N.P. Jayawardena[2], P.G.J.D. Kumarathunga[2], P.D.H. Dananjaya[2], E.A.C.P. Edirisinghe[2], M.D.N. Alwis[2], D.A. Daranagama[1]*, J.N. Dahanayake[2]* and C.C. Kadigamuwa[2]*

[1]*Department of Plant and Molecular Biology, University of Kelaniya, Kelaniya, Sri Lanka*

[2]*Department of Chemistry, University of Kelaniya, Sri Lanka*

Received: May 30, 2023; Accepted: October 28, 2023

ABSTRACT

This study is focused on determining the efficacy of natural compounds present in *Zingiber officinale* methanolic plant extraction in controlling seed-born fungal pathogens *Aspergillus flavus* and *Rhizopus oryzae*. The maximum percentage inhibition of 94.01% and 90.43% was reported against. *A. flavus* and *R. oryzae* respectively for the crude extract in the poison food agar method. These results were further confirmed by computational investigation. [4]-gingerol, [6]-gingerol, [8]-gingerol, [10]-gingerol, and [6]-dehydroginger phytochemicals identified in the extract were docked to the active sites in chitin synthase from *A. flavus* and squalene epoxidase from *A. flavus* and *R.oryzae,* and to the RNA dependent RNA polymerase (RdRp) enzyme from *R. oryzae*. The highest binding energy (BE) (-8.12 kcal/mol) was noticed between the interactions of squalene epoxidase and [6]-dehydroginger, and this complex was subjected to Molecular Dynamic (MD) analysis. MD simulations were performed on protein-ligand complexes for 10 ns using CHARMM36 force field. The mean radius of gyration (Rg), root mean square deviation (RMSD), and root mean square fluctuation (RMSF) were calculated and hydrogen bond analysis (HBA) was also performed. Rg and RMSD results indicated the stability of the protein-ligand complex throughout the simulation time.

Keywords: *Aspergillus flavus*, molecular docking, molecular dynamic, *Rhizopus oryzae Zingiber officinale*

INTRODUCTION

Sri Lanka's food supply revolves around cereal and legume crops centered on rice, and pulses followed by fruits and vegetables. South Asian nations underwent a dramatic transition in the second half of the 20th century as a result of the green revolution, which caused the production of cereal and legumes to many times. This highlighted the critical role that seeds play in the cultivation of approximately 90% of the world's food crops. The presence of external and internal seed-borne fungi causes negative effects like seed abortion, seed necrosis, loss of seed germination potential, and injury to seedlings (Mughal and Sers, 2020). These effects have been shown to have a major negative influence on agricultural productivity. In Sri Lanka, 46 different fungal species belonging to 26 different genera were reported on rice seeds (Bandara *et al.,* 2017). *Alternaria*, *Cercospora, Fusarium*, *Phytophthora*, and *Rhizoctonia* are the most common fungal pathogens associated with stored seeds. These fungal pathogens are mainly responsible for seed deterioration, reduction in germination potential, and seedling vigor (Chaudhari *et al.,* 2017). Fungal identification is highly involved in determining the most appropriate environmentally friendly

*Corresponding author's e-mail: cckadigamuwa@kln.ac.lk, jayangikadh@kln.ac.lk and anupamad@kln.ac.lk

approaches for controlling pathogens. Also, it is important to the implementation of necessary quarantine measures for disease management. Using fungicides is the usual chemical control method for seed-borne fungal pathogens.

However, due to these chemicals, resistant pathogen species are developed, and non-target environmental impacts are generated (Santini *et al.,* 2018). Therefore, using physical treatments such as bio-pesticides and natural plant extracts is comparatively eco-friendly (Sharaf and Al-Zaidi, 2021; Yasmeen *et al.,* 2020). The use of these natural extracts prevents the bio-deterioration of grains and also, avoids any toxic effect on the environment (Javed *et al.,* 2022).

Alternaria, *Aspergillus*, *Fusarium*, and *Penicillium* species have been reported as major contaminants of cereal grains. According to the Food and Agriculture Organization (FAO), mycotoxins are present in more than 25% of the world's foods (Reddy *et al.,* 2009). Mycotoxin contamination of cereal grain is a worldwide issue for public health and a permanent concern for cereal-food industries (Baliukonienė *et al.,* 2011). A permanent monitoring of mycotoxin content in cereals and maintaining and regulating the tolerable levels of mycotoxins are practiced worldwide for all the cereals and legumes accepted for human consumption (Tola and Kebede, 2016).

Computational studies have proven to be very useful in the design and discovery of novel medications for a variety of diseases (Rampogu *et al.,* 2018). In this study, the potential phytochemicals contained in the methanol extract of ginger were used to evaluate the antifungal activities against *A. flavus* and *R. oryzae* by *in silico* screening of phytochemicals contained in ginger, targeting RNA-dependent RNA polymerase, squalene epoxidase and chitin synthase protein using molecular docking and further, it was confirmed by molecular dynamics.

According to many researches, ginger root contains antifungal (Xi *et al.,* 2022), and antioxidant (Yousfi *et al.,* 2021) compounds, the most active of which are phenolic compounds such as shagelols, paradol, and gingerol (Rahmani *et al.,* 2014). The present study focuses on the inhibitory effects of five active polyphenolic compounds contained in ginger methanol extract, namely, 4-gingerol, 6-gingerol, 8-gingerol,10-gingerol and 6-dehydroginger on 3 main enzymes of *A. flavus* and *R. oryzae*. There are studies suggesting that due to their lipophilic properties, these compounds make both the fungal cell wall and cytoplasmic membrane more permeable by interacting with ergosterol, eventually leading to loss of cell integrity using *Aspergillus flavus* (Nerilo *et al.*, 2016; Sessou *et al.*, 2012).

The enzymatic composition of *Aspergillus flavus* and *R. oryzae* for the biosynthesis of ergosterol and chitin is of interest since these pathways are targeted for many antifungal drugs. Ergosterol is one of the most well-known sterols in the fungal cell membrane and it is synthesized from a highly conserved and complex pathway that can be studied using well-known *S. cerevisiae* as a model organism. In the early stage of the ergosterol biosynthesis pathway, two farnesyl-PP molecules are combined to form squalene by squalene synthase enzyme as the precursor. Squalene is then converted to lanosterol by the subsequent action of squalene epoxidase (Erg1) and the lanosterol synthase enzymes. Lanosterol is further converted to ergosterol through several intermediates by a specific mechanism that is different from *s. cerevisiae* depending on each fungal species (Jordá and Puig, 2020). When the allylamine group of antimycotics is used to disrupt this pathway, it is believed to inhibit Erg1 build up high intracellular squalene concentration, and obstruct fungal cell wall synthesis (Alcazar-Fuoli and Mellado, 2012).

Chitin biosynthesis happens via a process shared by all species capable of producing it. This process generally involves converting storage compounds such as glycogen and trehalose into linear chitin chains and for that different chitin synthases play a major role in different *Aspergillus* species. Chitin synthase (CS), a plasma membrane enzyme, uses UDP-N-GlcNAc as a substrate to transfer GlcNAc (N-acetylglucosamine) from UDP-GlcNAc to the developing chitin chains. It was discovered that CSs create a loop that serves as a gate, preventing the donor substrate from exiting the reaction site without being attached to a developing chitin oligomer. They also have the function of transporting new chitin chains to the extracellular space in the cell (Brauer *et al.,* 2023). Therefore, in this study, the activity of Squalene epoxidase and Chitin synthase enzyme is targeted for the inhibition of *Aspergillus flavus* by phytochemicals in ginger.

RNA-dependent RNA polymerase (RdRp) is a key fungal protein that is responsible for the replication and multiplication of RNAs from an RNA template strand in the

genome of many organisms including *R. oryzae*. Blocking this enzyme has been previously reported as a successful strategy to eradicate viral infections and therefore the same strategies are thought to be successful for fungal infections due to its highly conservative folds (Tian *et al.,* 2021).

This study is focused on determining the efficacy of natural compounds present in *Zingiber officinale* plant extract in controlling seed-borne fungal pathogens *Aspergillus flavus* and *Rhizopus oryzae*.

MATERIALS AND METHODS

Collection of samples

The *Zingiber officinale* rhizomes were collected from the market of Maharagama, Sri Lanka.

Methanol: Distilled water (4:1) extraction

Respective parts of *Z. officinale* rhizome 100 g were taken and thoroughly washed with tap water to remove soil and other dirt. Then the rhizomes were separated and air-dried under the shade at 25-29 °C until they became dry and crispy. The dried plant material was powdered by using a heavy-duty blender (Panasonic MX-AC 400-India). About 25 g of each air-dried plant material was defatted with n-hexane (C_6H_{14}) 10 mL volume. Then the solution was extracted with the methanol: distilled water (4:1) at room temperature (28±2 °C) by maceration with occasional stirring for 48 hours. The macerate was filtered using Whatman filter papers No. 1. Samples were concentrated by a rotary evaporator (IKA HB 10 digital-China) at 37 °C. Each sample was dissolved in Dimethyl Sulfoxide (DMSO) and DMSO-water (50%, V/V) was added to prepare the stock solutions (Chen *et al.,* 2019; Dehshahri *et al.,* 2012). Stock solutions were used to prepare the (10%, 15%, 20%) (w/v) solutions (Navoda and Anupama, 2022).

Antifungal activity by poison food method

Plant extract of *Z. officinale* was evaluated against the identified seed-borne pathogens including; *A. flavus* and *R. oryzae* (Ganeshalingam and daranagama, 2022). Plant extract at 10% (w/v), 15% (w/v), and 20% (w/v) concentrations were used for this study for which 10, 15, and 20 ml of stock solutions were mixed with 90, 85, and 80 ml of sterilized PDA media individually. The amended PDA medium was thoroughly shaken for uniform mixing with leaf extracts. 20 mL of this mixed agar media was poured into sterile Petri plates and allowed to solidify. Five mm of agar disk of test pathogenic fungi were cut from the 8-10 days old pure cultures using a sterile cork-borer and placed in the center of each Petri plate containing different concentrations of plant extracts. The experiment was carried out in triplicate (Ahmad *et al.,* 2016). The Petri plates with 10 mL of each solution including; fungicide 50% Captan, DMSO-water (50%, v/v), methanol-water (80%, v/v), sterilized distilled water, and n-hexane were mixed with 90 ml of sterilized PDA media and maintained as controls. Then the plates were incubated at room temperature (28±2 °C) for about seven days (Adeyemi *et al.,* 2018; Navoda and Anupama, 2022). At the end of the incubation period, the percentage inhibition of mycelial growth was calculated by using the below-mentioned equation (Ahmad and Pathak, 2016; Navoda and Anupama, 2022).

% inhibition effect = (Inhibition halo diameter in control – inhibition halo diameter in treatment) / (Inhibition halo diameter in control) x 100

Statistical analysis

All experiments were performed in triplicates and all the data were expressed as mean value ± (SE). Analysis of variance (ANOVA) and Tukey's multiple comparisons were performed on all transformed data collected concerning parameters studied on effects of plant extracts at the least significant difference (LSD) which was employed to test for significant differences between treatments at $P \leq 0.05$ using Minitab (version 17) (Navoda and Anupama, 2022).

Ligands preparation

At the initial, 3D conformations of the ligands were searched from PubChem and they were downloaded in SDF format file files. After that, these files were converted into the PDB format files. Then the above files were subjected to Avogadro software and the geometries were optimized by using Force Field MMFF94, algorithm steepest descent, 500 steps. Then the above files were saved as PDB format files and subjected to AutoDock Tools 1.5.6 and converted to PDBQT file formats.

Protein preparation

The protein uniport id of RNA-dependent RNA polymerase, Squalene epoxidase, and Chitin Synthase were obtained from the literature survey (Alcazar-Fuoli and Mellado, 2012; Brauer *et al.,* 2023; Jordá and Puig, 2020). Then the FASTA sequences of these proteins were aligned with the FASTA sequences of corresponding fungal proteins to check the similarity of the amino acids by using the UniProt server. FASTA sequences of these proteins were inserted into the BLAST server to find suitable templates (PDB ID). Then the same FASTA sequences of protein were inserted to search for suitable templates from the SWISS-MODEL server. The templates that had high coverage, and high GMQE (Global Model Quality Estimation) were selected as the good templates. By comparing these two methods, the most appropriate templates were identified and modeled via SWISS-MODELER. The energy optimization of the modeled proteins and the refinements were done by the Galaxy Refine webserver.

Model validation

The model proteins were validated by using Verify 3D, ERRAT, and PROCHECK via SAVES v6.0 server and ProSA server.

Binding site identification

The active site amino acids were determined via the CASTp server by uploading the refined PDB files to the server and the most probable active site amino acids were found.

Molecular docking

Water molecules were deleted, polar hydrogen atoms were added, and finally, Kollman chargers were added to the modeled protein structures using AutoDock Tools 1.5.6. Then the above files were saved as a PDBQT format file. By detecting torsion root using AutoDock Tools 1.5.6, ligand files were transformed to PDBQT format files. Both pdbqt files of ligands and protein were subjected to the AutoDock Tool 1.5.6. Grid parameter files were generated via Autogrid 4.2, while the Docking parameter files were generated by using AutoDock 4.2. The settings of the Lamarckian genetic algorithm (LGA) were adjusted as the number of genetic algorithms (GA) runs: 100, size of the population: 300, and 25000000 of maximum evaluations. Other parameters were kept as default. For this docking, site-specific docking was performed and rigid docking was done for all dockings, while macromolecules were kept as rigid and ligands kept as flexible. Finally, the resultant files were generated as (.dlg).

Analysis of docking results

To visualize the binding conformations of the protein and each ligand, Discovery Studio Visualizer and Ligplot software were used. Protein-ligand interaction profiler was used to validate the binding residues from the Discovery Studio Visualizer.

Molecular dynamic simulation

Protein-ligand complex with the best negative binding energies were selected to conduct molecular dynamics (MD) simulations to get further information regarding binding interactions between ligands and considered proteins and comparison of the protein-ligand complex. MD simulation of the above-mentioned protein-ligand complex was performed using the GROMACS (version 2021.4) software package and using the CHARMM36 force field with the TIP3P water model. While preparing the protein-ligand complex systems for the MD simulations, each complex was centered in a dodecahedron box with a minimum distance of 1.0 nm between the complex and any side of the box. The system was solved with water and Na^+ and Cl^- ions were added, replacing solvent molecules, to neutralize the systems at a 0.15 M salt concentration. In order to constraint bond lengths, the LINCS bond length constraint algorithm was used. Particle Mesh Ewald summation was used for electrostatic interactions and grid spacing of 0.12 nm combined with an interpolation order of 4 was used for long-range interactions. For van der Waals interactions, a cut-off of 1.4 nm was used. To perform energy minimization, the steepest descent algorithm was used. Then, the systems were gradually heated from 50 K to 300 K throughout a 100 ps time frame. Final production runs for MD were done in the NPT ensemble for 10 ns at 300 K using a V-rescale thermostat and at 1 bar using Berendsen barostat. The trajectories obtained from MD simulations were used to calculate the radius of gyration (Rg), root mean square deviation (RMSD), and root mean square fluctuation (RMSF).

RESULTS

Antifungal activity of *Zingiber officinale* methanol extract against *A. flavus*, and *R. oryzae*

Methanol extract of *Zingiber* officinale at all three concentrations 10%, 15%, and 20% (w/v), significantly reduced the mycelial growth of tested pathogens (Table 1). The level of controlling seed-born fungal pathogens by three different concentrations of *Z. officinale* extract, 10% (w/v), 15% (w/v), and 20% (w/v) was statistically significant ($P<0.05$) compared to the negative controls (0%). The effect of crude extract of *Z. officinale* in inhibiting the seed-borne fungal pathogens was considerably higher than the other concentrations. The inhibition of *A. flavus* and *R. oryzae* was found to increase with the concentration of plant extraction in the poisoned food technique. The methanolic extracts of *Z. officinale* showed the most significant antifungal activity against the selected pathogens in this study. The maximum percentage inhibition of 94.01% was recorded for *A. flavus* by *Z. officinale* methanolic crude extract.

Table 1: Percentage inhibition effect of different concentrations of Zingiber officinale extract against the A. flavus, and *R. oryzae* after 7 days of incubation (10%, 15%, and 20% indicate 10% (w/v), 15% (w/v), and 20% (w/v) concentration, Crude extract indicates 100% concentration without dilution, Captan 50% indicates positive control). (Solutions with concentrations of 10% (w/v), 15% (w/v), and 20% (w/v) were prepared using a stock solution that was prepared with Dimethyl Sulfoxide (DMSO) and DMSO-water (50%, v/v)).

Percentage inhibition (%)	***Zingiber* officinale extraction concentration (w/v)**					
± standard error	**Negative control**	**10%**	**15%**	**20%**	**Crude extraction**	**Captan (50%)**
Aspergillus flavus	$0.00^{j}\pm0.00$	$70.98^{i}\pm1.60$	$78.81^{h}\pm2.01$	$87.56^{d,e,f}\pm0.80$	$94.01^{a,b,c}\pm1.66$	$98.16^{a}\pm0.47$
Rhizopus oryzae	$0.00^{j}\pm0.00$	$77.03^{h}\pm1.11$	$78.31^{h}\pm2.78$	$85.97^{e,f,g}\pm1.28$	$90.43^{b,c,d,e}\pm1.10$	$94.26^{a,b}\pm0.00$

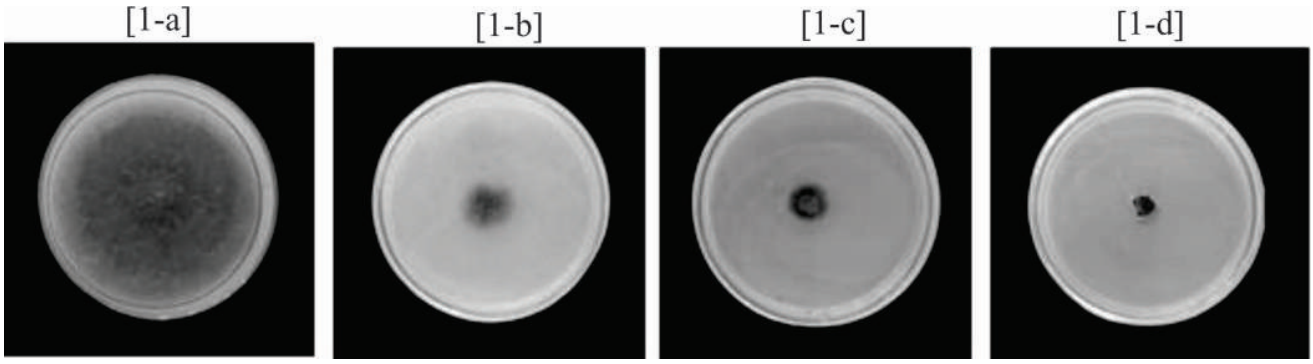

Figure 1: Effect of different concentrations of *Z. officinale* extract against the selected seed-borne pathogen; *A. flavus* **1a** *A. flavus* in negative control (Distilled water); **1b** *A. flavus* in 20% concentration; **1c** *A. flavus* in crude extract **1d** *A. flavus* in Captan 50 % positive control.

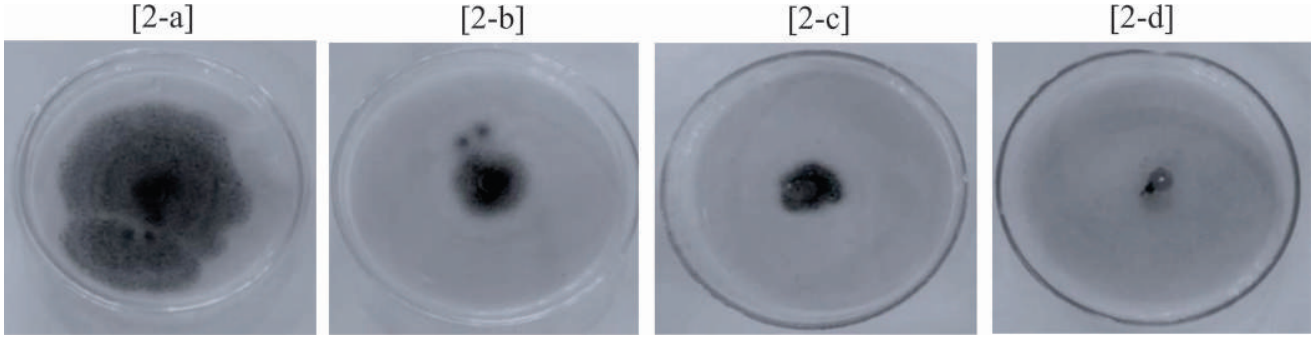

Figure 2: Effect of different concentrations of *Z.* officinale extract against the selected seed-borne pathogen; *R. oryzae* **2a** *R. oryzae* in negative control (Distilled water); **2b** *R. oryzae* in 20% concentration; **2c** *R. oryzae* in crude extract **2d** *R. oryzae* in Captan 50% positive control.

Ligands identification

Based on literature reviews, 5 phytochemicals were identified which were able to extract into methanol from ginger. Those phytochemicals were filtered based on their percentage amount extracted into methanol. They are [4]-gingerol, [6]-gingerol, [8]-gingerol, [10]-gingerol, and [6]-dehydroginger (Jiang *et al.,* 2005).

Protein Models validation

After the energy optimization, all the selected proteins proceeded to ERRAT, VERYFY 3-D, PROCHECK, and ProSA servers. The VERYFY 3-D score gives the matching of an atomic 3D model with its 1D peptide sequence by determining the structural class. Modeled protein, which has an 80.00% overall quality score, is considered a good model. Among the analyzed proteins, this value varied between 80% to 95%. ERRAT server interprets the statistics of non-bound interactions between atom types. The acceptable value of ERRAT is greater than 60. According to the results, this value was in the range of 47%-75% for all proteins. PROCHECK server was used to examine the placement of amino acid residues in the permitted and forbidden zones, and also the protein structure's overall stereochemical quality. It gives the geometry of the protein with the Ramachandran plot calculations. Ramachandran plot gives the possible Psi and Pi angles for amino acids. Accordingly, all proteins' amino acid residues in the favored region were high and they were above 90.0%. The residues in additional allowed regions, generously allowed regions, and disallowed regions were low. ProSAweb server is used to check the potential errors of the 3D structure of the protein. Z score from this server gives the total quality of the model. In addition, it gives the total energy of the 3D structural protein compared to energy variation from random conformations. Negative values of the z score represent the protein validity. In selected proteins, this z-score value changed from -5.05 to -8.98, which confirmed the validity of proteins. All the results are summarized in (Table 2).

Molecular Docking Analysis

Five ligands were docked to the binding pockets identified from the CASTp web server. According to the docking results (Table 3) were obtained for the site-specific docking of [4]-gingerol, [6]-gingerol, [8]-gingerol, [10]-gingerol, and [6]-dehydroginger phytochemicals contained in the ginger methanol extract to the active sites in Chitin Synthase from *Aspergillus flavus* and Squalene epoxidase protein from *Aspergillus flavus* and *R. oryzae,* and to the RNA dependent RNA polymerase (RdRp) enzyme from *R. oryzae*. The highest binding energy (BE) (-8.12 kcal/mol) was given between the interactions of Squalene epoxidase and [6]-dehydroginger and it was subjected to molecular dynamic analysis after the confirmation of interactions between the

Table 2: Modeled proteins validation results

Model Description	RNA-dependent RNA polymerase	Squalene epoxidase	Chitin synthase
Ramachandranp lot			
Residues in most favored regions [A, B, L]	362 (92.3%)	281 (90.9%)	545 (94.3%)
Residue in additional allowed regions [a,bl,p]	26 (6.6%)	24 (7.8%)	27 (4.7%)
Residues in generously allowed regions [~a,~b,~l,~p]	0 (0.0%)	2 (0.6%)	4 (0.7%)
Residues in disallowed regions	4 (1.0%)	2 (0.6%)	2 (0.3%)
Number of non-glycine and non-proline residues	392 (100%)	309 (100%)	578 (100%)
Number of end-residues (excl. Gly and Pro)	2	2	2
Number of Glycine residues	23	28	45
Number of Proline residues	31	26	23
Total number of residues	448	365	648
ERRAT overall quality score	80.98	90.03	95.02
VERIFY 3-D (3D-1D score >0.2)	47.40%	75.62%	53.70%
ProSA Z-score	-6.67	-8.98	-5.05

Table 3: Docking results of crystal structure of three different fungus proteins with curry powder ligands

Protein	Phytochemicals	Binding energy (kcal/mol)
RNA-dependent RNA	4-gingerol	-6.97
polymerase	6-dehydroginger	-7.24
	6-gingerol	-7.44
	8-gingerol	-5.63
	10-gingerol	-5.73
Chitin Synthase	4-gingerol	-7.15
	6-dehydroginger	-7.08
	6-gingerol	-7.37
	8-gingerol	-6.22
	10-gingerol	-6.88
Squalene Epoxidase	4-gingerol	-7.05
	6-dehydroginger	-.8.12
	6-gingerol	-7.03
	8-gingerol	-6.87
	10-gingerol	-7.87

ligand and the protein from protein-ligand interaction profiler, LigPlot server and Discovery studio visualizer. Additionally, binding energies of 13 proteins-ligand interactions were greater than (-6.00 kcal/mol) out of 15 docking results. All the phytochemicals, which were docked to Chitin Synthase and Squalene epoxidase proteins from *Aspergillus flavus,* had shown values above -6.00 kcal/mol. Hence, more negative energies mean that this ginger extract has a higher anti-fungal effect.

Proteins and ligands interactions analysis

It was noted that binding energy alone cannot predict the effect on the target protein function. The binding pocket's location, non-covalent interactions, hydrogen bond interactions, salt bridges, and their types of amino acids have to be considered before making conclusions. To understand better, the relationships between complexes that showed the greatest binding energies, each complex was evaluated further using the protein-ligand interaction

Table 4: Amino acids involved in ligand-protein interactions (binding energy greater than (-6.00 kcal/mol)) including the types of interactions that each amino acid favors. Each interactions are represented by **hydrophobic interactions**, *hydrogen bondings*, hydrophobic interactions+ H bondings-*, hydrophobic interactions+π stackings, and ***π stackings*** respectively

Protein	Phytochemicals	Binding Energies (kcal/mol)	Amino acids responsible for ligand-protein interactions
RNA-dependent RNA polymerase	4-gingerol	-6.97	**Pro806**, *Gln820*, **Val823, Ala826**, *Arg860,* **Ile867, Leu875**
RNA-dependent RNA polymerase	6-dehydroginger	-7.24	**Ile805, Val827, Arg860, Tyr863, Ile867, Gln874, Leu875, Leu878,** *Leu818*
RNA-dependent RNA polymerase	6-gingerol	-7.44	**Pro806, Val823, Ala826**, Arg860*, **Ile867, LEU871, Leu878,** *Gln820*
Chitin Synthase	4-gingerol	-7.15	Lys318*, Tyr460, **Tyr460, Leu461, Arg506, Asn509,** *Leu447, Arg505, Asp715*
Chitin Synthase	6-dehydroginger	-7.08	**Lys318,** Lys319*, Leu320*, Tyr460, **Glu463**, *Leu447, His448, His714*
Chitin Synthase	6-gingerol	-7.37	Lys318*, **Leu320,** Tyr460, **Leu461, Arg506, Asn509**, *His714, Asp715, Tyr784*, ***His448***
Chitin Synthase	8-gingerol	-6.22	Lys318*, **Leu320,** Tyr460, **Leu461, Arg506, Asn509**, *His714, Asp715, Tyr784,* ***His448***
Chitin Synthase	10-gingerol	-6.88	**Leu320, Tyr460, Glu463***, Lys319, Tyr441, Asp464,* ***Trp507***
Squalene Epoxidase	4-gingerol	-7.05	**Glu70, Leu71, Phe100**, Tyr239, **Gln240, Leu249**, *Ser97, Pro325*
Squalene Epoxidase	6-dehydroginger	-8.12	**Glu70, Leu71, Phe100, Leu237, Tyr239, Gln240**, *Ser97, Pro325*
Squalene Epoxidase	6-gingerol	-7.03	Glu70*, Leu71*, Phe100, **Leu237, Tyr239, Leu249,** *Tyr113*
Squalene Epoxidase	8-gingerol	-6.87	**Glu70, Leu71, Phe100**, Tyr113*, *Ser127,* ***Tyr239***
Squalene Epoxidase	10-gingerol	-7.87	Glu70*, **Leu71, Phe100, Leu237, Tyr239, Leu249**, Arg323*, **Pro325,**

profiler (Table 4), LigPlot server and Discovery studio visualizer. According to the analysis of interactions between proteins and ligands using the above-mentioned methods, [4]-gingerol, [6]-gingerol, [8]-gingerol, [10]-gingerol, and [6]-dehydroginger phytochemicals were bound to the amino acids included in the binding pockets of three proteins which were determined from the CASTp server. 2D and 3D visualizations of LigPlot server (Figure 3) and Discovery studio visualizer (Figure 4) were depicted below only for the 6-dehydroginger-squalene epoxidase complex.

In this study, molecular dynamic simulations were done for the 6-dehydroginger squalene epoxidase complex and the results were sufficient enough to prove the protein-ligand interaction stability. When concerning the cellular mechanism, in the presence of high binding energy and strong interactions with the binding pocket amino acids of

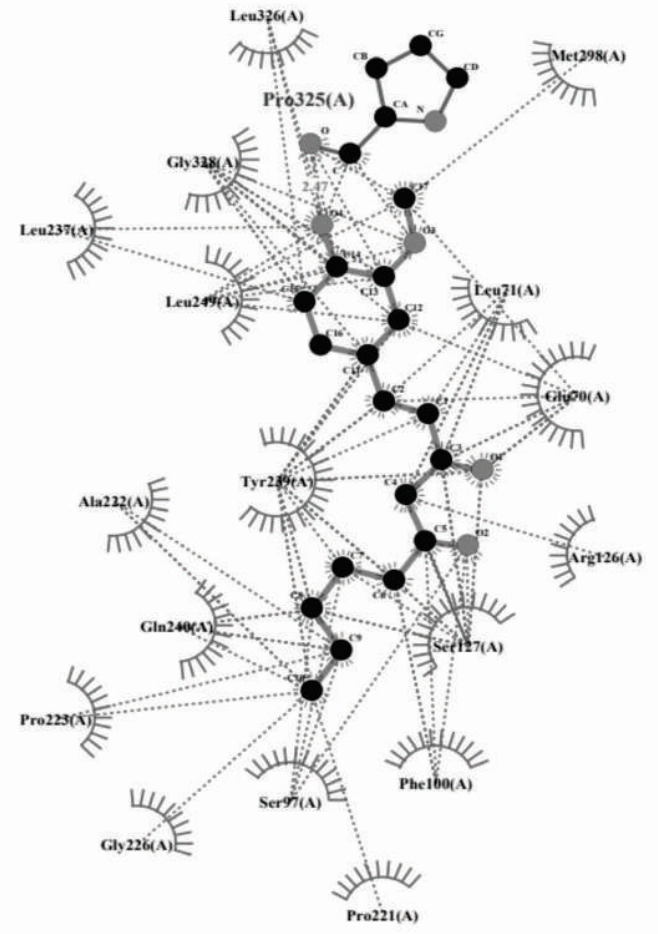

Figure 3: 2D visualization of protein-ligand complex of 6-dehydroginger-squalene epoxidase

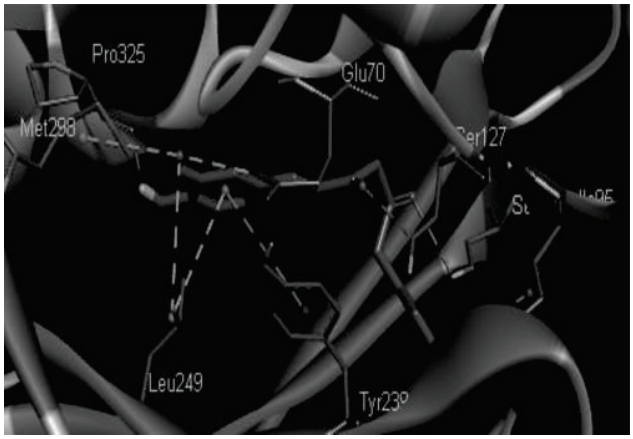

Figure 4: 3D visualization of protein-ligand complex of 6-dehydroginger-squalene epoxidase

squalene epoxide, the conversion of squalene to squalene epoxide could be affected by the [6]-dehydroginger ligand. Because of that metabolism and cellular biochemical pathways have been disrupted and obstructed fungal cell wall synthesis.

MD results analysis

Although the binding energies, amino acids, and the types of interactions between the binding pockets of the protein-ligand complexes were obtained using docking results but the stability of these complexes and their flexibility are still unknown. Therefore, in this research, the stability of the ligands to a protein was investigated using MD simulations. To carry out MD simulation, the protein-ligand complex with highest binding energy was considered. According to (Table 4), (SQ)-6-dehydroginger complex accounts for the MD simulation due to having -8.12 kcal/mol of binding energy. MD simulations measure particle interactions as a function of their individual substituent particles' coordinates. To analyze the confirmational variations throughout the simulation time, it is important to consider the results from the root mean square deviation (RMSD), radius of gyration (Rg), and root mean square fluctuation (RMSF).

Radius of gyration (Rg)

Rg is a parameter that shows how the protein structure compactness changes over time in a simulation. It's about how normal secondary structures can be compactly packed into a protein's 3D structure. The Rg was also calculated to

see whether the complexes were folded or unfolded properly after the MD simulation. SQ with 6HD complex does not show significant fluctuations and indicates that SQ with 6HD is stable throughout the simulation time. The graph of Rg as a function of time for SQ-6HD complex is shown below (Figure 5).

Root mean square deviation (RMSD)

RMSD is a useful method for determining how proteins change their conformation. The RMSD is determined by rotating and converting the instantaneous structures' coordinates to superimpose them with the reference structure with the greatest overlap. According to the RMSD graph of SQ-6HD complex, throughout simulation time from 0 to 10ns, around ~0.35 nm value flattening curve indicated its stability when it is compared with the initial input SQ-6HD complex. Therefore, this complex was stable throughout the simulation (Figure 6).

Root mean square fluctuation (RMSF)

The RMSF is a measure of a single atom or a group of atoms displacement from the reference structure, averaging over the number of atoms. RMSF values of the protein-ligand complex reveal the effect of dynamic movements of residues. In RMSF, it computes the fluctuations of each amino acid residues relative to the simulation's average structure when a simulation is equilibrated, or when the structure of interest fluctuates around a stable average conformation. The variations in the constituent residues in the protein-ligand complex, and the flexibility of each residue in the protein-ligand complex result in the plot after the simulation period. According to the SQ-6HD RMSF plot analysis, the residues that show high fluctuations between ~0.30 nm and ~0.50 nm do not contribute to the interaction with 6HD because these residues generate protein structure

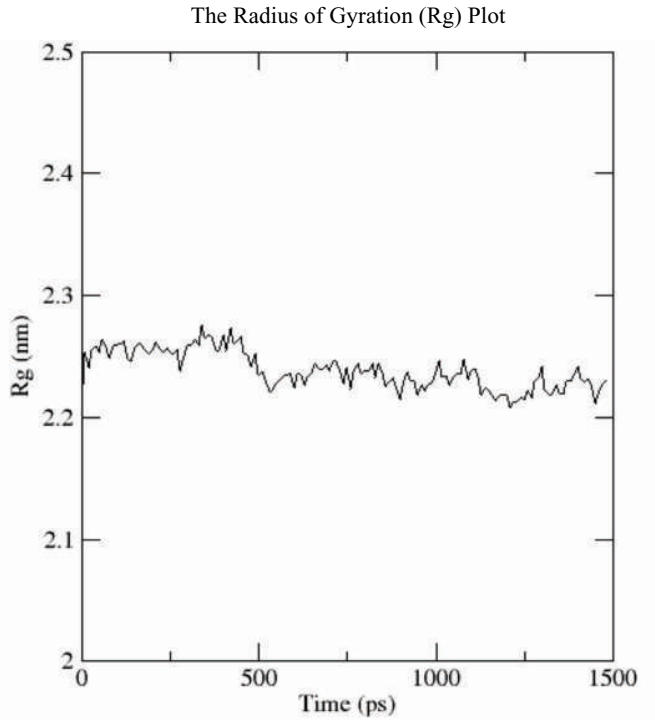

Figure 5 : The radius of gyration plot of SQ-6HD complex

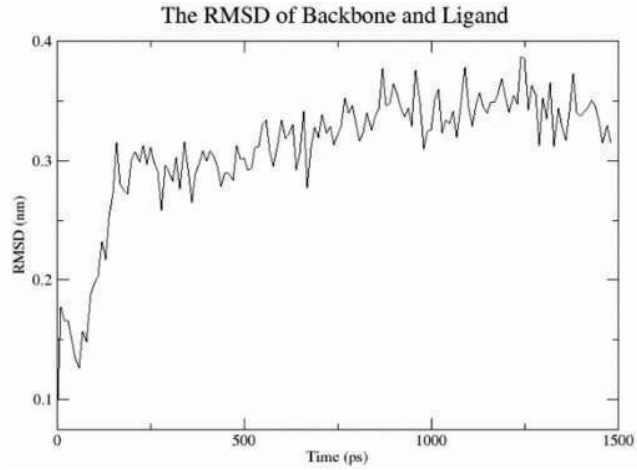

Figure 6: The Root mean square deviations (RMSD) plot of SQ-6HD complex

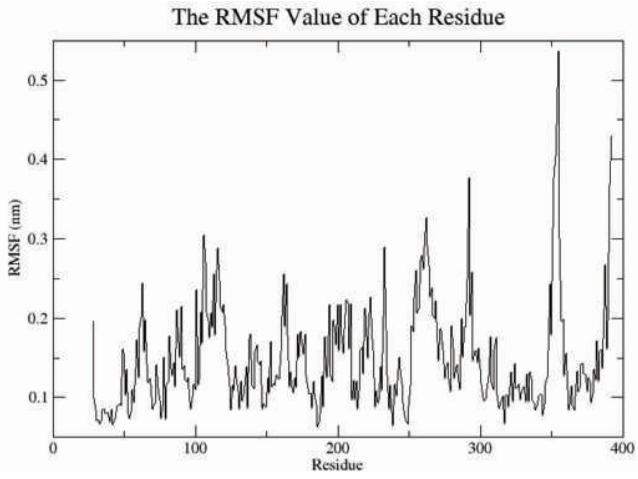

Figure 7 : The Root mean square fluctuation (RMSF) plot of SQ-6HD complex

fluctuation or a large portion of protein fluctuation. Remain residues fluctuate significantly around ~0.15 nm, which indicates the involvement of the SQ-6HD complex in the interaction (Figure 7).

DISCUSSION

A. flavus and *R. oryzae* fungal pathogens are mainly responsible for seed deterioration, reduction in germination potential, and seedling vigor. These effects have been shown to have a major negative influence on agricultural productivity in Sri Lanka. Therefore, it becomes essential to design drugs against *A. flavus* and *R. oryzae* with minimum or no side effects. In this manuscript, we have made an effort to test some methanolic extractable natural compounds of *Z. officinale* against these fungal strains and to determine the most probable targets of those compounds in the pathogens.

Agar well diffusion assay is the most commonly used method to determine the antimicrobial activity of plant extracts (Faden, 2018). Also, it is one of the official methods used in many clinical microbiology laboratories for routine antimicrobial susceptibility testing. However, this approach is reliant on the inhibitory substance diffusing through the agar, which could be influenced by the size, medium components, and fungi-secreted compounds which could react (Arena *et al*., 2016). The antimicrobial ingredient diffuses across the agar medium and prevents the growth of microbial strains tested. When comparing the two approaches (agar well diffusion and poison food technique) utilized in the current study to assess the *in vitro* activity of plant extracts in reducing seed-borne fungal infections, it is noteworthy to mention that the poison food technique exhibited a rather significant effect in inhibition. Furthermore, in the poisoned food technique plant extracts were mixed with the PDA before the PDA medium solidified which enhances the proper interaction of plant extract with the agar medium and facilitates a considerable diffusion (Musa *et al*., 2022). According to Samawaty *et al.* (2021) the most effective antifungal components in *Z. officinale* were identified to be gingerol, cedrene, and zingiberene, which play critical roles in common fungal mycelial growth suppression.

Many scientists have discovered the value of using several extracts to evaluate the efficacy of plants for antimicrobial activity in a variety of plant species, which is relevant to the present study. The aqueous extracts of *Z. officinale* had strong antifungal activity against the fungus *A. niger* and 100% enhance the germination of *O. sativa* (Sreelakshmi and Bindu, 2018). Furthermore, *Z. officinale* was found highly effective in reducing the growth of the seed-borne fungus and enhancing seed germination (Jatoi *et al*., 2019). Similar results show that the alcoholic extract has the best antimicrobial activity and it was also reported by Jasicka-Misiak *et al*. (2018). This showed that methanol helped to extract the phenolic compounds more effectively from the *A. sativum* plant. The *A. sativum* is reported to be rich in active phenolic compounds (Parvu et al., 2019). Also, n-hexane helped to extract the organosulfur compounds present in the *A. sativum*, most prominently allicin (Laokor and Juntachai, 2021).

A precise mechanism of the squalene epoxidase inhibition has been shown *in silico* approaches by establishing an atomic-resolution model of the yeast *Saccharomyces cerevisiae* with the aid of the 3D-Jury technique, a fully atomic three-dimensional (3D) model of the squalene epoxidase (EC 1.14.99.7) from *S. cerevisiae* was created, and it was then further screened using information from mutation trials that resulted in terbinafine resistance. The mechanism of interaction between terbinafine and squalene epoxidase was identified by docking investigations, molecular dynamics simulations, and quantum interaction energy calculations. According to the results, it was notified that terbinafine and SE interact with each other most strongly when Tyr90's hydroxyl group and terbinafine's amine nitrogen atom form hydrogen bonds. These findings, which provide light on the molecular basis of terbinafine's inhibitory effect, can be used to develop more potent or targeted antifungal medications or even pharmaceuticals that lower cholesterol in people (Nowosielski *et al.,* 2011).

Moreover, in a study 2014, the homology model and the structure-based pharmacophore model of *Candida albicans* squalene epoxidase (CASE) were built respectively. The active site of CASE was docked with three typical SE inhibitors (Naftifine, Terbinafine, Butenafine). The investigation of the inhibitor binding mode and the distribution of pharmacophore characteristics were then

used to create the novel SE inhibitors. These substances underwent additional synthesis and *in vitro* testing. They showed some antifungal action, particularly the molecule phenylmethanamine, which also significantly inhibits resistant fungus. Further investigation revealed that the substance phenylmethanamine, which is related to naftifine, could inhibit SE. The work demonstrated the logic of molecular models, which can be used to build and find more effective antifungal SE inhibitors (An *et al.,* 2020).

Another *in silico* study was conducted on antifungal targets like Squalene epoxidase (SE) and 14-demethylase (CYP51), several active fragments were screened using the De Novo Link method, and those active fragments with higher Ludi_Scores were chosen because they can demonstrate their ability to bind to both SE and CYP51 targets. By joining these core pieces, three series of target compounds with naphthyl amide scaffolds were created, and their structures were synthesized. These target substances can obstruct the manufacturing of ergosterol by blocking the action of dual targets (SE, CYP51) according to preliminary mechanistic research (An *et al.,* 2021).

In addition to that, *in silico* antibacterial activity of *zingiber officinale* has been reported in a previous study, where the interaction between c-Jun NH2-terminal kinases (JNKs) and phytol chemical present in the methanol extract of the *Z. officinale* was analyzed computationally. Based on the results, phytol showed strong interaction with the JNKs with a binding energy of -7.48 Kcal/mol (Biochemical *et al.,* 2018).

According to previous studies, many chemical compounds have been derivatized to produce antifungal drugs. Naftifine and Terbinafine are the widely used drugs against squalene epoxidase of the fungus (Xi *et al.,* 2022). Terbinafine (Lamisil) inhibits squalene epoxidase specifically, which gives it a fungicidal effect on a variety of fungi which suppress the enzyme action in a non-competitive way (Ryder, 1992). In addition to the above mentioned drugs, fluconazole, itraconazole, voriconazole, posaconazole, carbendazim, and ravuconazole are utilizing to disrupt the metabolism of the squaline epoxidase (Sayed *et al.,* 2014). Out of these fungicides, carbendazim was approved by the ISO with the common name methyl 2-benzimidazole carbamate and this fungicide is a systemically active benzimidazole that prevents the formation of beta-tubulin. When concerning the above-discussed details, fungal squalene epoxidase enzyme has been already tested to inhibit cell wall synthesis by disrupting the conversion of squalene to squalene-epoxide.

The poisoned food technique was carried out to examine the antifungal properties against *A. flavus* and *R. oryzae* fungal strains and to determine the effectiveness of natural chemicals found in the methanolic plant extract of *Zingiber officinale* in managing the seed-borne fungi. Pathogen growth was inhibited significantly by *Z. officinale* methanol extract at 10%, 15%, and 20% (w/v) concentrations for *A. flavus* and *R. oryzae,* respectively However, the maximum percentage inhibition of 94.01% and 90.43% was reported for *A. flavus* and *R. oryzae* for the *Z. officinale* crude extract. These results were further proven by computational investigation.

[4]-gingerol, [6]-gingerol, [8]-gingerol, [10]-gingerol, and [6]-dehydroginger phytochemicals present in this extract were docked to the active sites in chitin synthase from *A. flavus* and squalene epoxidase from *A. flavus* and *R. oryzae,* and to the RNA dependent RNA polymerase (RdRp) enzyme from *R. oryzae*. According to docking studies, binding energies of 13 proteins-ligand interactions were greater than (-6.00 kcal/mol) out of 15 docking results. All the phytochemicals, which were docked to chitin synthase and squalene epoxidase proteins from *A. flavus* had shown values above -6.00 kcal/mol. The highest binding energy (BE) (-8.12 kcal/mol) was given between the interactions of squalene epoxidase and [6]-dehydroginger. According to the obtained results for Squalene epoxidase and [6]-dehydroginger complex, Ser 97 and Pro 325 were involved to form Hydrogen bonds with the [6]-dehydroginger ligand while other amino acids formed the hydrophobic interactions. When concerning the interacting position of the ligand, the hydrophobic chain with carbonyl groups of the ligand bound to Glu70, Leu71, Phe 100, Tyr, Glu 240, and Ser97. Leu 237 and Pro 325 interacted with the 6-membered and the R group of the cyclic 5-membered part of the ligand respectively. Hence, these results indicated that the stability of squalene epoxidase and [6]-dehydroginger and this complex were subjected to Molecular Dynamic (MD) analysis. The mean radius of

gyration (Rg), root mean square deviation (RMSD), and root mean square fluctuation (RMSF) were calculated and hydrogen bond analysis (HBA) was also performed. Rg and RMSD results indicated the stability of the protein-ligand complex throughout the simulation time and thereby, it can be concluded that [6]-dehydroginger has the potential to be utilized as a potential antifungal source against *Aspergillus flavus* and *Rhizopus oryzae* fungal strains.

CONCLUSION

In this study, methanolic extract of the *Zingiber officinale* was able to control the growth of the analyzed pathogens in the presence of 10%, 15%, and 20% (w/v) concentrations. The maximum inhibitions of 94.01% and 90.43% were observed for *A. flavus* and *R. oryzae.* When considering the computational results, the highest binding energy (-8.12 kcal/mol) was given between the squalene epoxidase and [6]-dehydroginger with strong H bondings, and the conformational behaviors were revealed through the MD studies. The MD analysis results along with the docking results indicated that the above-mentioned [6]-dehydroginger with higher binding affinity has the potential to obstruct *Aspergillus flavus* and *Rhizopus oryzae* cell wall synthesis by disrupting the conversion of squalene to squalene-epoxide. Further molecular dynamics analysis needs to be carried out to study the behavior of each protein-ligand complex and their interactions. Solvent accessible surface area (SASA) should also be carried out to measure the proportion of the protein surface which is accessible to the water solvent, and this parameter could be used to predict the extent of the conformational changes that occurred during protein-ligand interactions. In addition to that principal component analysis (PCA) can be carried out to investigate the collective motion of the protein-ligand complexes and this analysis method could be used to retrieve Gibb's free energy landscape to predict the stability of each protein–ligand complex. Along with these two methods, free energies of interaction responsible for the protein-ligand binding can be calculated using the Parrinello-Rahman parameter of GROMACS. Furthermore, the ultimate goal of our study was to use *Zingiber officinale* plant extraction against these pathogenic fungi in order to use them as a successful natural fungicidal agent.

ACKNOWLEDGEMENTS

We thank the Department of Chemistry, and Plant and Molecular Biology, University of Kelaniya, Sri Lanka for providing some of the instruments for the experiments. Funds for research are provided by the faculty of science University of Kelaniya, Sri Lanka by the Research Grant RP/03/02/06/06/2021.

Conflict of interest

Authors have no conflict of interest to declare.

REFERENCES

Adeyemi AI, Vincent OI and Olujenyo OM (2018). Phytochemical screening and antifungal activity of *Chromolaena odorata* extracts against isolate of *Phytophthora megakarya* using agar-well diffusion method. *Asian J. Med. Biol. Res.,* 4(1): 7–13.

Ahmad L and Pathak N (2016). Antifungal potential of plant extracts against seed-borne fungi isolated from barley seeds (*Hordeum vulgare* L.). *J. Plant Pathol. Microbiol.*, 7(5): 1-4.

Alcazar-Fuoli L and Mellado E (2012). Ergosterol biosynthesis in *Aspergillus fumigatus*: Its relevance as an antifungal target and role in antifungal drug resistance. *Front. Microbiol.,* 3: 1–6.

An Y, Dong Y, Liu M, Han J, Zhao L and Sun B (2021). Novel naphthylamide derivatives as dual-target antifungal inhibitors: Design, synthesis and biological evaluation. *Eur. J. Med. Chem.,* 21(2): 143-149.

An Y, Dong Y, Min L, Zhao L, Zhao D, Han J and Sun B (2020). Construction and evaluation of molecular models: guide and design of novel SE inhibitors. *ACS Med. Chem. Lett.,* 11(6): 1152–1159.

Arena MP, Silvain A, Normanno G, Grieco F, Drider D, Spano G and Fiocco D (2016). Use of *Lactobacillus plantarum* strains as a bio-control strategy against food-borne pathogenic microorganisms. *Front. Microbiol.,* 7(3): 464-474.

Baliukonienė V, Bakutis B, Januskevicienė G and Miseikienė R (2011). *Fungal contamination* and *Fusarium mycotoxins* in cereals grown in different tillage systems. *J. Anim. Feed Sci.,* 20(4): 637–647.

Bandara MMK, Herath HMVG, Wickramasinghe HAM and Bamunuarachchige TC (2017). Assessment of morphological characters of selected traditional Sri Lankan rice varieties *(Oryza sativa L.)*. *J. Dryland Agric.,* (3): 21-28.

Benkerroum N (2020). Chronic and acute toxicities of aflatoxins: Mechanisms of action. *Int. J. Environ. Res. Public Health.,* 17(2): 1–28.

Brauer VS, Pessoni AM, Freitas MS, Cavalcanti-Neto MP, Ries LNA and Almeida F (2023). Chitin biosynthesis in *Aspergillus species*. *J. Fungus,* 9(1): 1–42.

Chaudhari A, Sharma H, Jehani M and Sharma JK (2017). Seed mycoflora associated with pigeonpea [*Cajanus cajan* (L.) Millsp.], their significance and the management. *J. Pure App. Microbiol.,* 11(1): 567–575.

Chen J, Shen Y, Chen C and Wan C (2019). Inhibition of key citrus postharvest fungal strains by plant extracts *in vitro* and *in vivo*: A review. *Plants,* 8(2): 1–19.

Deepa S and Boominathan M (2018). *In silico* determination and biological evaluation of methanol extract of *Zingiber officinale* S. *Asian J. Innov. Res.,* 3(1): 27–33.

Dehshahri S, Wink M, Afsharypuor S, Asghari G and Mohagheghzadeh A (2012). Antioxidant activity of methanolic leaf extract of *Moringa peregrina* (Forssk.) Fiori. R*es Pharm Sci.,* 7(2): 111–118.

Denardi-Souzaa T, Luzb C, Mañesb J, Badiale-Furlonga E and Meca G (2018). Antifungal effect of phenolic extract of fermented rice bran with *Rhizopus oryzae* and its potential use in loaf bread shelf life extension. *J. Sci. Food Agric.,* 98(13): 5011–5018.

Faden AA (2018). Evaluation of antibacterial activities of aqueous and methanolic extracts of *Areca catechu* against some opportunistic oral bacteria. *Biosci. Biotechnol. Res.,* 15(3): 655-659.

Ganeshalingam A and Daranagama DA (2022). First comprehensive study on distribution frequency and incidence of seed-borne pathogens from cereal and legume crops in Sri Lanka. *Phytotaxa.,* 531(3): 267-281.

Jasicka-Misiak I, Poliwoda A, Petecka M, Buslovych O, Shlyapnikov VA and Wieczorek PP (2018). Antioxidant phenolic compounds in *Salvia officinalis* L. and *Salvia sclarea* L. *Ecol. Chem. Eng.,* 25(1): 133 -142.

Jatoi GH, Keerio AU, Abdulle YA and Qiu D (2019). Effect of selected fungicides and bio-pesticides on the mycelial colony growth of the *Helminthosporium oryzae* brown spot of rice. *Acta Ecol. Sin.,* 39(6): 456-460.

Javed A, Shahid MB, Naeem H, Jam AH, Nawaz A and Nazeer A (2022). Aflatoxins poisoning. *Haya: Saudi J. Life Sci.*, 7(2): 34–37.

Jiang H, Sólyom AM, Timmermann BN and Gang, DR (2005). Characterization of gingerol-related compounds in ginger rhizome (*Zingiber officinale* Rosc.) by high-performance liquid chromatography/electrospray ionization mass spectrometry. *Rapid Commun. Mass Spectrom.*, 19(20): 2957–2964.

Jordá T and Puig S (2020). Regulation of ergosterol biosynthesis in saccharomyces cerevisiae. *Genes*, 11(7): 1–18.

Laokor N and Juntachai W (2021). Exploring the antifungal activity and mechanism of action of *Zingiberaceae* rhizome extracts against *Malassezia furfur. J. Ethnopharmacol.,* 279: 114354-114361.

Mdee LK, Masoko P and Eloff JN (2009). The activity of extracts of seven common invasive plant species on fungal phytopathogens. *S. Afr. J. Bot., 75*(2): 375–379.

Mohana DC, Thippeswamy S, Abhishek RU, Shobha B and Mamatha MG (2017). Studies on seed-borne mycoflora and aflatoxin B1 contaminations in food based seed samples: Molecular detection of mycotoxigenic *Aspergillus flavus* and their management. *Int. Food Res. J.,* 24(1): 422–427.

Mughal and Fontan Sers C (2020). Cereal production, undernourishment, and food insecurity in South Asia. *Rev. Dev. Econ.*, 24(2): 524–545.

Musa FM, Haruna NFG, Nuhu AM, Ibrahim B and Abdulkadir S (2022). Antimicrobial activity of *Mitracarpus scaber* leaf extract against some human pathogenic microorganisms. *Afr. Health Sci.,* 22(1): 23-30.

Navoda H and Anupama DD (2022). Evaluation of antifungal plant extracts against cereal and legume seed-borne pathogens for effective management. *Stud. Fungi,* 7(9): 1-11.

Nelson S (2009). Rhizopus Soft Rot of Sweetpotato. *Plant Dis.,* pp 1–5.

Nerilo SB, Rocha GHO, Tomoike C, Mossini SAG, Grespan R, Mikcha JMG and Machinski M (2016). Antifungal properties and inhibitory effects upon aflatoxin production by *Zingiber officinale* essential oil in *Aspergillus flavus*. *Int. J. Food Sci. Technol.,* 51(2): 286–292.

Nowosielski M, Hoffmann M, Wyrwicz LS, Stepniak P, Plewczynski DM, Lazniewski M, Ginalski K and Rychlewski L (2011). Detailed mechanism of squalene epoxidase inhibition by terbinafine. *J. Chem. Inf. Model,* 51(2): 455–462.

Parvu M, Mot CA, Parvu AE, Mircea C, Stoeber L, Rosca-Casian O and Tigu AB (2019). *Allium sativum* extract chemical composition, antioxidant activity and antifungal effect against *Meyerozyma guilliermondii* and *Rhodotorula mucilaginosa* causing onychomycosis. *Molecules,* 24(21): 3958-3975.

Rahmani AH, Al Shabrmi FM and Aly SM (2014). Active ingredients of ginger as potential candidates in the prevention and treatment of diseases via modulation of biological activities. *Int. J. Physiol. Pathophysiol. Pharmacol.,* 6(2): 125–136.

Rampogu S, Baek A, Gajula RG, Zeb A, Bavi RS, Kumar R, Kim Y, Kwon YJ and Lee KW (2018). Ginger (*Zingiber officinale*) phytochemicals-gingerenone-A and shogaol inhibit SaHPPK: Molecular docking, molecular dynamics simulations and *in vitro* approaches. *Ann. Clin. Microbiol. Antimicrob.*, 17(1): 1–15.

Reddy KRN, Reddy CS and Muralidharan K (2009). Detection of *Aspergillus* spp. and aflatoxin B1 in rice in India. *Food Microbiol*., 26(1): 27–31.

Ryder N (1992). Terbinafine: Mode of action and properties of the squalene epoxidase inhibition. *Br. J. Dermatol.,* 39(1): 2–7.

Samawaty AERM, El-Wakil DA, Alamery S and Mahmoud MM (2021). Potency of plant extracts against *Penicillium species* isolated from different seeds and fruits in Saudi Arabia. *Saudi J. Biol. Sci.,* 28(6): 3294-3302.

Santini A, Liebhold A, Migliorini D and Woodward S (2018). Tracing the role of human civilization in the globalization of plant pathogens. *ISME J.,* 12(3): 647–652.

Sayed MA, Hassaneen HM, Kholy AA and Naguib RM (2014). Effect of fluconazole and terbinafine on the activities of lanosterol 14 α-demethylase and squalene epoxidase in ergosterol biosynthetic pathway. *Egypt J. Bot.,* 54(2): 247–262.

Sessou P, Farougou S and Sohounhloué D (2012). Major component and potential applications of plant essentials oils as natural food preservatives : A short review research results. *Int. J. Biosci.,* 2(8): 45–57.

Sharaf EF and Al-Zaidi HS (2021). *In vitro* antifungal activity of some indigenous medicinal plant extracts against five isolates of *Aspergillus fumigatus*. *Indian J. Pharm. Sci.*, 83(4): 695–700.

Sreelakshmi VV and Bindu R (2018). Seed-borne fungi associated with some stored seeds and their bio-control by aqueous medicinal plant extract. *Sci.,* 14(1): 58-63.

Tian L, Qiang T, Liang C, Ren X, Jia M, Zhang J, Li J, Wan M, YuWen X, Li H, Cao W and Liu H (2021). RNA-dependent RNA polymerase (RdRp) inhibitors: The current landscape and repurposing for the COVID-19 pandemic. *Eur. J. Med. Chem.,* 213: 113201.

Tola M and Kebede B (2016). Occurrence, importance and control of mycotoxins: A review. *Cogent Food Agric*., 2(1): 1-12.

Xi KY, Xiong SJ, Li G, Guo CQ, Zhou J, Ma JW, Yin JL, Liu YQ and Zhu YX (2022). Antifungal activity of ginger rhizome extract against *Fusarium solani*. *Horticulturae.*, 8(11): 1-19.

Yasmeen R, Gul R and Mazhar S (2020). Antifungal activity of onion and garlic extract for the control of *Aspergillus niger* isolated from Ghurki Village. *LGU J. Life Sci.*, 2(4): 258–267.

Yousfi F, Abrigach F, Petrovic JD, Sokovic M and Ramdani M (2021). Phytochemical screening and evaluation of the antioxidant and antibacterial potential of *Zingiber officinale* extracts. *S. Afr. J. Bot.,* 142: 433–440.